

## **CHAPTER 3**

### **EXPERIMENTAL PROCEDURE**

This thesis has the main purpose to fabrication of dense nanocrystalline HA ceramic. This title mentions 3 properties of the materials to be fabricated. First of all, the HA is nanopowder and should be synthesized with simple method for the largely mass product in the shorting times. Second requirement is a density of sintered HA at least 95%. The third and most important one is the requirement of nanoscale dimensions for microstructure, these mean grains of HA nanoceramic or nanocomposites should have structural feature with at least one dimensions in the nano-domain, which is in between 1 and 100 nanometer.

#### **3.1 Synthesis of nanocrystalline hydroxyapatite powder**

The hydroxyapatite powder was derived from natural bovine bone by a sequence of thermal processes. The fresh bones from all parts of one cow were cut into smaller pieces and cleaned well to remove macroscopic adhering impurities. The bone samples were boiling in distilled water for 8 h for easy removal of the bone marrow and tendons. After that the bone has been deproteinized by continued boiling in water. The boiled bone samples were then dried overnight at a temperature of 200 °C. The deproteinized bone was calcined at 800°C for 3 h, a temperature at which no prions or any disease-causing agents can survive. The resulting product was crushed into small pieces and milled in a ball mill pot for 24 h. Each 20 g of dried powders

were reground by vibro-milling method with various milling time of 0, 1, 2, 4 and 8 h, respectively. The phase identification and particle size of as-prepared powders have been examined via X-ray diffraction techniques. For the microstructural analysis, the dried powder were mounted on stubs, gold-coated in vacuum and viewed under scanning electron microscope. Moreover, the energy dispersive X-ray analyser (EDS) was employed for phase quantitative analysis. The nanopowder sample was ultrasonically dispersed in ethanol to form very dilute suspensions and then a few droplets were put on copper grids coated with carbon film for further examination by transmission electron microscopy. The crystallographic information could be examined by transmission electron diffraction (TED) pattern.

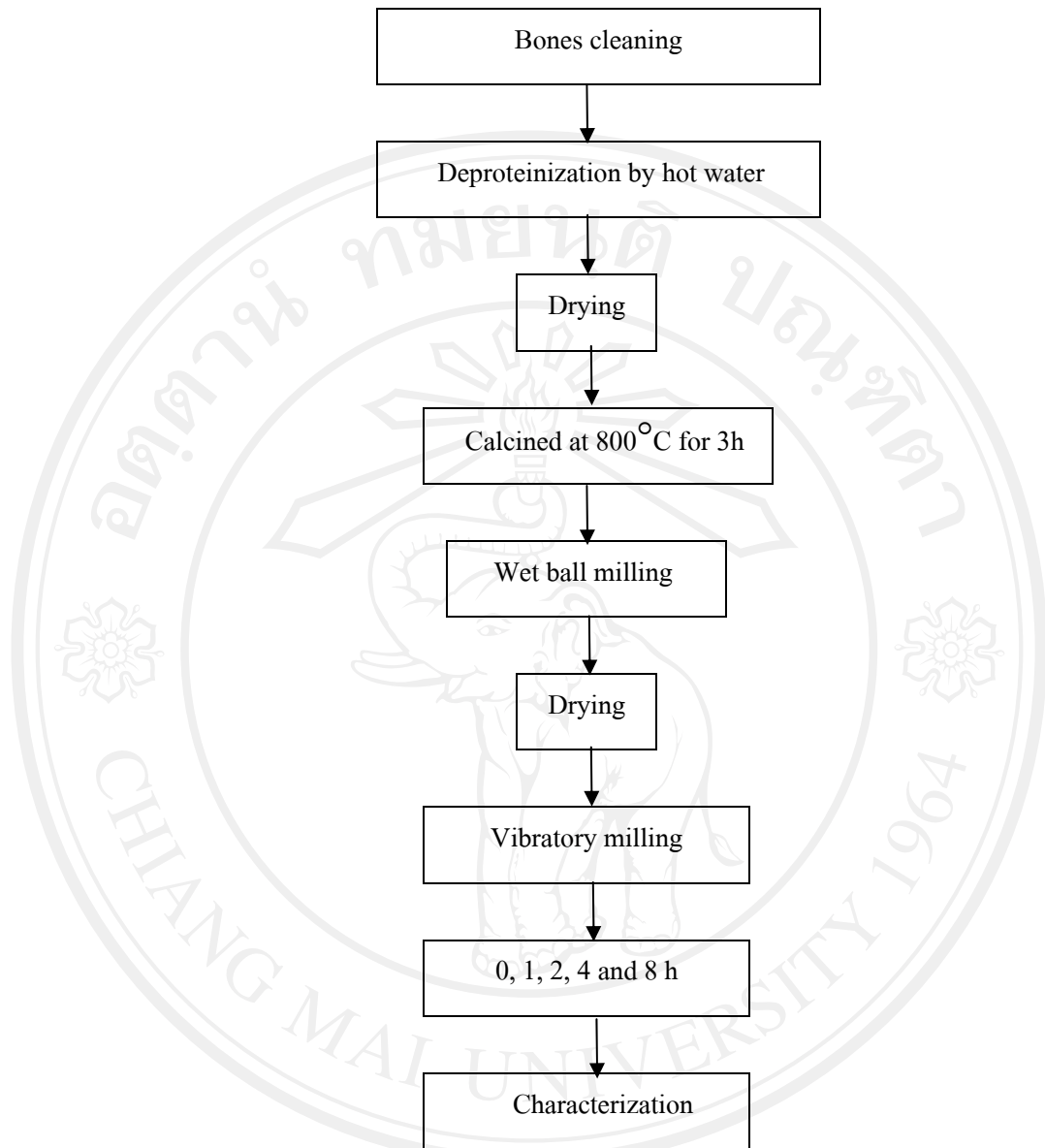


Fig. 3.1 A diagram of preparation of nanocrystalline hydroxyapatite powder

### **3.2. Synthesis of SiO<sub>2</sub> nanopowder from rice husk ash**

To confirm that vibro-milling method is a beneficial process to produce the nanopowders of low cost and high mass productivity. The rice husk ash was chosen for synthesis SiO<sub>2</sub> nanopowder as a comparative study.

The rice husk grains were washed with distilled water to remove adhering soil and dust. The rice husk samples were firing at 1000°C for 3 h in electrical furnace to form RHA. The resulting product was milled in a ball mill pot for 24 h. The dried powders were reground by vibro-milling method for 4 h. The product was heat treated at 1000°C for 3 h to eliminate carbonaceous material. Quantitative chemical analyze of as-prepared powder was accomplished by X-ray fluorescence (XRF). The phase evolution was investigated by X-ray diffraction technique (XRD). The powders were mounted on stubs, gold-coated in vacuum and viewed under scanning electron microscope (SEM).

### **3.3 Experimental procedure**

#### **3.3.1 Thermally stability of nanocrystalline hydroxyapatite powder**

The nanocrystalline HA powder of 4 h vibro-milling times were calcinations in air at temperatures range between 1000 and 1300°C, at a heating rate of 4°C/min and soaking time of 3 h. The thermogravimetric analyser (TGA) was performed to analyze the phase transition. Phase stability and microstructure evolution were determined by X-ray diffraction (XRD) and scanning electron microscopy (SEM).

### **3.3.2 Sintering of HA nanopowders with conventional sintering**

The agglomerate HA powders of all vibro-milling times were pressed into pellets at a pressure of 50 MPa and sintered in air atmosphere at 1200°C and 1300°C with 3 h soaking time and a heating rate of 4 °C/min. Density and open porosity of the sintered samples were measured by the Archimedes' method with distilled water as the fluid medium. The microstructure and fracture surface analysis of the sintered HA ceramics were carried out using the scanning electron microscopy and the X-ray diffractometer, respectively. Hardness test was carried out in Vickers microhardness tester with major load of 0.98 N for 15 s. The flexural bending strength of the samples was obtained by ball-on-ring test method using universal testing machine with constant crosshead speed of 5 mm/min. A set of six samples were tested and the average values were reported in all tests.

### **3.3.3 Sintering of HA nanopowders with rate-controlled sintering**

The nano HA powders of 4 h vibro-milling times have been pressed into discs at a pressure of 50 MPa. The simplest sintering method was used pressureless sintering at temperatures varying from 1150°C, 1200°C, 1250°C and 1300°C for 3 h by different two sintering techniques. One, the green compacts were sintered with linear heating rate of 4 °C/min and the second sintering techniques were used non-linear heating rate sintering (see Fig. 3.2). At least 6 samples of the same composition were prepared for each sintering conditions. Density and open porosity of the sintered samples were measured by the Archimedes' method with distilled water as the fluid medium. The microstructure of fracture surface analysis of sintered HA ceramics were carried out using scanning electron microscopy.

A 9.8 N load was applied for 15 s using a pyramid shaped diamond indenter was indented 20 times used to determine hardness.

The flexural bending strength of samples was obtained by ball-on-ring test method using universal testing machine with constant crosshead speed of 5 mm/min.

### 3.3.4 Fabrication of craniotomy flap fixation plates

The nano HA powders have been pressed into pellet shape by uniaxial pressing with pressure of 50 MPa. The circular green HA disks were perforated at the center as to form the button shape. The simplest sintering method was used for pressureless sintering at temperatures of 1200°C for 3 h with rate control (see Fig 1(b)). Density and open porosity of the sintered samples was measured by the Archimedes' method with distilled water as the fluid medium. The microstructure and fracture surface analysis of sintered HA ceramics were carried out using scanning electron microscopy.

Fracture toughness ( $K_{1C}$ ) was determined by an indentation technique and calculated employing Anstis' equation<sup>16,21-23</sup>:

$$K_{1C} = 0.016 \left( \frac{E}{H} \right)^{1/2} \frac{P}{c^{3/2}} \quad (3.1)$$

Where  $c$  is the crack length (m),  $E$  is the Young's modulus (GPa),  $H$  is the hardness (GPa),  $P$  is the load applied (N).

A 9.8 N load was applied for 15 s with a pyramid shaped diamond indenter and the samples were indented 20 times. These indentations were also used to determine hardness.

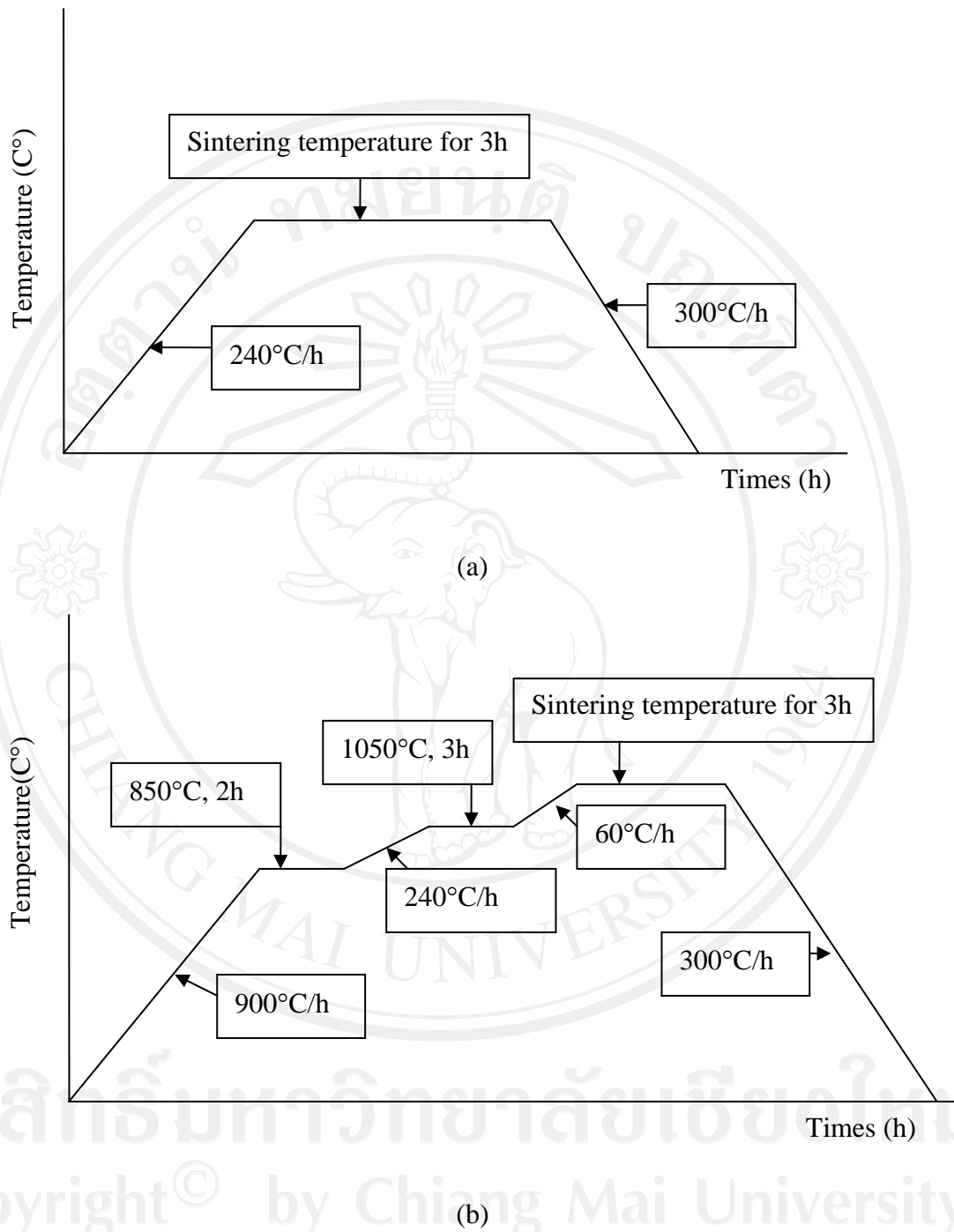


Fig. 3.2 Difference two sintering methods (a) linear heating rate sintering and (b) non-linear heating rate sintering.

### 3.3.5 Fabrication of Nanoporous HA ceramics

The hydroxyapatite powder was derived from extracted deproteinized bovine bone with calcinations at 800°C for 3 h. After that it was crushed to small pieces and milled in a ball mill pot for 24 h and then sieved to obtain average particle size of smaller than 45  $\mu\text{m}$ . The composite was obtained by mixing PVA powder with hydroxyapatite powder in a wt ratio of 40:60 and ball milled in ethanol for 24 h, dried and sieved. Nanosized HA nanocomposite particles were prepared by vibro-milling method for 4 h. The powder was uniaxial pressed in a stainless steel mold. The product was sintered at 1200°C for 3 h with heating rate of 4°C/minute. The thermal stability was characterized by X-ray diffraction (XRD). The nanoporous structure was examined using scanning electron microscopy (SEM). The physical properties of porosity and bending strength were investigated by the Archimedes' method and ball-on-ring test, respectively.

### 3.4 Structural characterization

X-ray diffractometry (XRD: Philip X'pert) was used for identifying the crystalline phase of  $2\theta$  at 0.01°C/min from 20° to 60°.

For the microstructural analysis, the dried powder were mounted on stubs, gold-coated in vacuum and viewed under scanning electron microscope (SEM:JSM-6335F). Moreover, the energy dispersive (EDS) was employed for phase quantitative analysis.

The nanopowder sample was ultrasonically dispersed in ethanol to form highly dilute suspensions and then a few droplets were put on copper grids coated with carbon film for further examining by the transmission electron microscopy



(CM20 TEM/STEM). The crystallographic information could be examined by transmission electron diffraction (TED) pattern.

Thermo-gravimetric analysis (TGA) was carried out on calcined powder, using alumina powder as reference material on a Pyris Diamond simultaneous TG/DTA apparatus (Perkin-Elmer make, model SII) from 40 to 1200°C in nitrogen atmosphere.

### 3.5 Physical characterization

#### 3.5.1 Density and porosity

##### *Apparent density*

This is the ratio of the mass of a material to its apparent volume, i.e. the volume of material plus the volume of sealed pores.

##### *Bulk density*

This is the ratio of the mass of a material to its bulk volume, i.e. the volume of material plus all its pores. It is also known as ‘apparent specific gravity’

##### *Porosity*

Apparent porosity is the ratio of volume of the open pores to the bulk volume of a material.

Density and open porosity of the sintered samples were measured by the Archimedes’ method with distilled water as the fluid medium. If

$W_{\text{dry}}$  = weighed of dry test piece;

$W_{\text{sat}}$  = weighed of test piece soaked and suspended in the immersion liquid;

$W_{\text{sup}}$  = weighed of test piece soaked and suspended in air;

$\rho_{H_2O}$  = density of water at temperature of 21.5°C is 0.997879 g/cm<sup>3</sup>.

then

$$\text{Apparent density} = \left( \frac{W_{dry}}{W_{dry} - W_{sup}} \right) \rho_{H_2O} \quad (3.2)$$

$$\text{bulk density} = \left( \frac{W_{dry}}{W_{sat} - W_{sup}} \right) \rho_{H_2O} \quad (3.3)$$

$$\text{Apparent porosity} = \left( 1 - \frac{\text{bulk density}}{\text{apparent density}} \right) 100 \quad (3.4)$$

### 3.6 Mechanical characterization

#### 3.6.1 Hardness

The microhardness of the samples was measured with a Vickers microhardness tester. The sample was subjected to diamond indenter with a 1 kg load was pressed into a sample. Approximately 20 indented positions were performed on each sample. The hardness values were obtained via calculation employing the equation.

$$HV = 1.854 \frac{P}{d_i^2} \quad (3.5)$$

Where HV: Vickers hardness, P (kg): applied load, d (mm): diagonal indent length.

#### 3.6.2 Bending strength

The bending strength of the samples was measured with a ball-on-ring test<sup>33</sup>. The ball-on-ring test was performed using a biaxial flexure jig as shown in Fig. 3.3. The bending strength values were calculated from equation 3.6.



Fig. 3.3 The ball-on-ring tests

$$\sigma_{\text{Max}} = \frac{3F(1+\nu)}{4\pi^2} \left[ \frac{(1-\nu)}{(1+\nu)} \cdot \frac{(2a^2 - b^2)}{2R^2} + 2\ln\left(\frac{a}{b}\right) + 1 \right] \quad (3.6)$$

Where;

$\sigma_{\text{Max}}$  is the maximum stress in MPa

F is the breaking load in Newton

$\nu$  is Poisson's ratio

a is the radius of supporting ring

R is the radius of the samples

t is thickness

b is  $t/3$

### 3.6.3 Fracture toughness

Indentation tests are widely used for evaluating the fracture toughness of dense bioceramic materials and a great number of equations have been proposed for the calculation using Vickers indentation<sup>16,50</sup>. These equations either consider that the crack emanating from the indentation is of mean half-penny shape<sup>50</sup>.

Fracture toughness ( $K_{1C}$ ) was determined by an indentation technique as Anstis, according to following equation (3.1)<sup>16,21-23</sup>:

$$K_{1C} = 0.016 \left( \frac{E}{H} \right)^{1/2} \frac{P}{c^{3/2}}$$

Where  $c$  is the crack length (m),  $E$ , the Young's modulus (GPa),  $H$ , the hardness (GPa),  $P$ , the load applied (N).

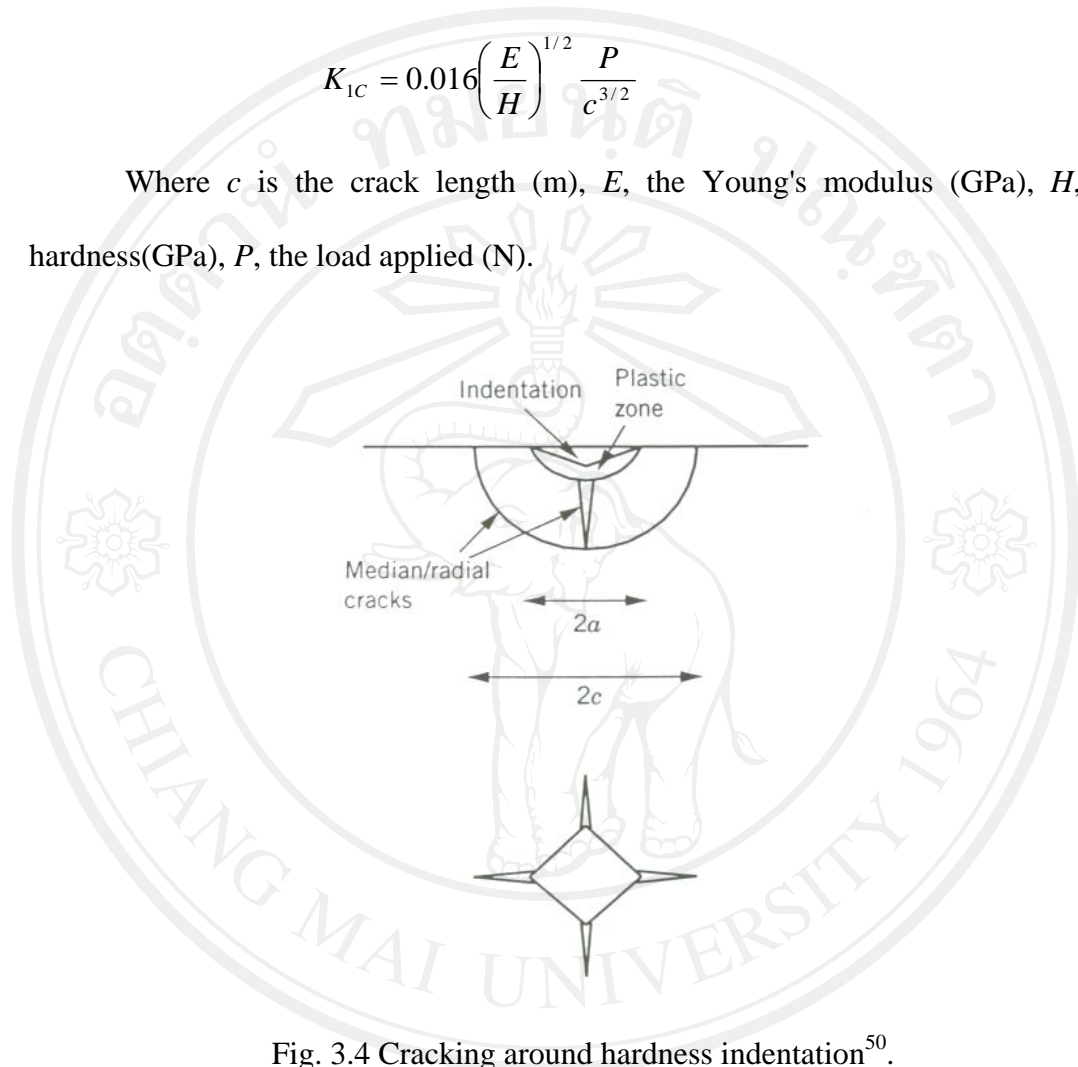


Fig. 3.4 Cracking around hardness indentation<sup>50</sup>.